

# The Bremsstrahlung Process $\nu_\tau \rightarrow \nu_e e^+ e^- \gamma$

H. Schmid and G. Raffelt

*Max-Planck-Institut für Physik (Werner-Heisenberg-Institut), Föhringer Ring 6, 80805 München, Germany*

A. Leike

*Ludwig-Maximilians-Universität, Sektion Physik, Theresienstr. 37, 80333 München, Germany*  
(April 20, 1998)

The bremsstrahlung process  $\nu_\tau \rightarrow \nu_e e^+ e^- \gamma$  is the dominant photon-producing decay of heavy  $\tau$  neutrinos with  $m_{\nu_\tau} > 2m_e$  so that this process is instrumental for supernova 1987A constraints on the properties of these particles, notably on their mixing amplitude with  $\nu_e$ . We calculate the rate of the bremsstrahlung process as well as the photon spectrum and the angular distribution relative to the spin direction of the parent neutrino. We carefully pay attention to the difference between Dirac and Majorana neutrinos.

PACS numbers: 14.60.Pq, 14.60.Lm, 13.35.Hb, 97.60.Bw

## I. INTRODUCTION

The direct experimental limits on neutrino masses are so crude that astrophysical arguments remain the most important source of information on their possible magnitude. The well-known cosmological limit [1]  $m_\nu \lesssim 40$  eV improves the experimental  $m_{\nu_\tau}$  limit of about 18.2 MeV [2] by almost six orders of magnitude, assuming that it is stable on cosmological time scales. This longevity cannot be taken for granted because the standard-model decay  $\nu_\tau \rightarrow \nu_e e^+ e^-$  is fast on cosmic time scales even for relatively small mixing angles between  $\nu_\tau$  and  $\nu_e$ . Therefore, to plug this loophole on the cosmological  $m_{\nu_\tau}$  limit, one needs restrictive limits on the  $\nu_e$ - $\nu_\tau$  mixing angle. Even then, of course, heavy  $\tau$  neutrinos could decay fast by new interactions so that the cosmological mass bound is never absolute. In fact, heavy  $\nu_\tau$ 's with “invisible” fast decays can fix certain problems of the standard cold dark matter cosmology, leading to the interesting class of cosmological  $\tau$ CDM models [3]. In any case, proving that a heavy  $\nu_\tau$  requires interactions beyond the particle-physics standard model to escape the cosmological mass limit is a significant constraint on its possible properties.

If  $\nu_e$  and  $\nu_\tau$  mix with each other, any  $\nu_e$  source also produces a certain  $\nu_\tau$  flux. Experimental limits on the flux of decay electrons and positrons from beam-dump [4], reactor [5], and solar neutrinos [6] provide strong limits on the mixing amplitude. The most restrictive limit arises from core-collapse supernovae which are powerful  $\nu_\tau$  sources because they produce this flavor directly rather than by an assumed mixing with  $\nu_e$ . The decay positrons would linger in the galaxy for about  $10^5$  years until they annihilate so that one can derive restrictive limits on the  $\nu_\tau \rightarrow \nu_e e^+ e^-$  channel from the

observed interstellar positron flux [7–9]. In addition, the absence of  $\gamma$ -rays associated with the neutrino burst from supernova (SN) 1987A provides further limits where the bremsstrahlung process  $\nu_\tau \rightarrow \nu_e e^+ e^- \gamma$  is the dominant photon-producing reaction [8–11].

This literature has two important gaps. First, no detailed calculation of  $\nu_\tau \rightarrow \nu_e e^+ e^- \gamma$  is available. While the simple estimates used in Refs. [8–11] are certainly adequate for a first estimate, a detailed calculation of the expected  $\gamma$ -ray spectrum from a supernova depends on the angular distribution and spectrum of the photons in a given  $\nu_\tau \rightarrow \nu_e e^+ e^- \gamma$  decay. It is the purpose of our paper to provide this missing calculation.

A second gap concerns the data used for the derivation of the limits. Refs. [8–10] used  $\gamma$ -ray data that had been taken by the Gamma Ray Spectrometer on the Solar Maximum Mission satellite in coincidence with the SN 1987A neutrino signal. Ref. [11] used  $\gamma$ -ray data from the Pioneer Venus Orbiter spacecraft that were also taken in coincidence with the SN 1987A burst. However, to constrain radiative decays from MeV-mass neutrino decays it is not critical to use data even close to the  $\bar{\nu}_e$  burst because the expected  $\gamma$  pulse is widely dispersed. The COMPTEL instrument aboard the Compton Gamma Ray Observatory satellite looked at the SN 1987A remnant for about  $0.68 \times 10^6$  s in 1991 [12], much longer than the previous experiments. Because of the long COMPTEL viewing period, one could derive limits on the  $\nu \rightarrow \nu' \gamma$  channel which are far superior to the SMM and PVO results, assuming that the neutrino mass exceeds about 0.1 MeV [12]. For smaller masses the  $\gamma$  burst would have ended before COMPTEL looked at the SN so that the previous limits remain of interest. In the  $\nu_\tau \rightarrow \nu_e e^+ e^-$  scenario it is necessarily assumed that  $m_{\nu_\tau} \gtrsim 1$  MeV so that the COMPTEL limits are

naturally the most restrictive. However, the authors of Ref. [12] have only analysed the direct channel  $\nu_\tau \rightarrow \nu_x \gamma$ . Our bremsstrahlung calculation could be used to extend the interpretation of the COMPTEL data to the more interesting  $\nu_\tau \rightarrow \nu_e e^+ e^- \gamma$  case.

Aside from the practical application in the supernova context, the bremsstrahlung process turns out to be another interesting example for the differences between massive Dirac and Majorana neutrinos.

We proceed in Sec. II with a brief discussion of the bare process  $\nu_\tau \rightarrow \nu_e e^+ e^-$ . In Sec. III we calculate the rate, spectrum, and angular distribution of the bremsstrahlung process  $\nu_\tau \rightarrow \nu_e e^+ e^- \gamma$ . In Sec. IV we discuss and summarize our results.

## II. THE BARE PROCESS

We begin with a discussion of the bare decay process  $\nu_3 \rightarrow \nu_1 e^+ e^-$  where we assume a neutrino mass hierarchy of the form  $m_3 > m_2 > m_1$ . The  $m_3$  eigenstate is taken to be the dominant admixture of the  $\nu_\tau$  flavor eigenstate, and similarly  $m_1$  is the dominant mass component of the electron neutrino. This process is then essentially what we sloppily called  $\nu_\tau \rightarrow \nu_e e^+ e^-$  in the introduction.

For a Dirac neutrino the relevant amplitude is the tree-level graph of Fig. 1(a) which was evaluated by Shrock [13]. The decay rate is found to be

$$\begin{aligned} \Gamma_{\text{bare}} &= |U_{e3}U_{e1}|^2 \frac{G_F^2}{3(4\pi)^3} m_3^5 \Phi(m_3) \\ &= |U_{e3}U_{e1}|^2 3.5 \times 10^{-5} \text{ s}^{-1} \left( \frac{m_3}{1 \text{ MeV}} \right)^5 \Phi(m_3), \quad (1) \end{aligned}$$

where  $U_{e1}$  and  $U_{e3}$  are the mixing amplitudes between  $\nu_e$  and  $\nu_1$  or  $\nu_3$ , respectively, and  $G_F$  is Fermi's constant. It was assumed that  $m_1$  is negligibly small. The phase-space factor (Fig. 2) is

$$\begin{aligned} \Phi(m_3) &= (1 - 4a)^{1/2} (1 - 14a - 2a^2 - 12a^3) \\ &+ 24a^2(1 - a^2) \ln \frac{1 + (1 - 4a)^{1/2}}{1 - (1 - 4a)^{1/2}} \quad (2) \end{aligned}$$

with  $a \equiv (m_e/m_3)^2$ .  $\Phi$  approaches unity for  $m_3 \gg m_e$ .

This process was also studied by Li and Wilczek [14] with an emphasis on the difference between Dirac and Majorana neutrinos. Following their treatment we note that for Majorana neutrinos the decay rate is effectively

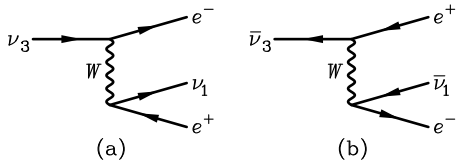


FIG. 1. Decay amplitude for a heavy neutrino.

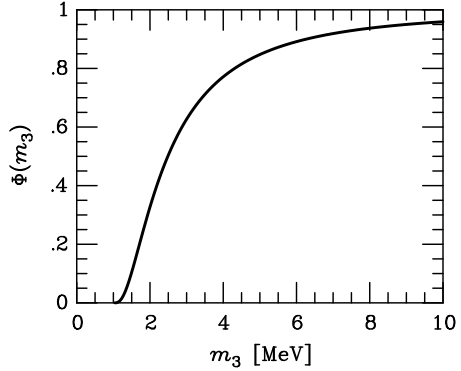


FIG. 2. Phase-space factor according to Eq. (2).

the incoherent sum of the two Dirac graphs depicted in Figs. 1(a) and (b). While Li and Wilczek focussed on the angular distribution of the final-state charged leptons and did not explicitly compare the absolute rates, their treatment implies that the Majorana decay rate is twice the Dirac one, a result which we also find by an independent evaluation of the relevant S-matrix element. The phase-space factor of Eq. (2) is the same in both cases.

If  $\nu_3$  is a Dirac neutrino the normalized positron and electron spectra  $dN/dE_\pm = \Gamma_{\text{bare}}^{-1} d\Gamma_{\text{bare}}/dE_\pm$  are

$$\begin{aligned} \frac{dN}{dE_+} &= \Theta(q^2 - m_e^2) \frac{96}{m_3^5} \frac{(E_+^2 - m_e^2)^{1/2}}{\Phi(m_3)} f(q^2) q^2 E_+, \\ \frac{dN}{dE_-} &= \Theta(q^2 - m_e^2) \frac{32}{m_3^5} \frac{(E_-^2 - m_e^2)^{1/2}}{\Phi(m_3)} f(q^2) \\ &\times \left[ \frac{q^2 - m_e^2}{2} E_- \right. \\ &\left. + \frac{q^2 + 2m_e^2}{q^2} (m_3 - E_-) (m_3 E_- - m_e^2) \right], \quad (3) \end{aligned}$$

where  $q^2 = m_3^2 - 2m_3 E_\pm + m_e^2$  and  $f(q^2) = (1 - m_e^2/q^2)^2$ .

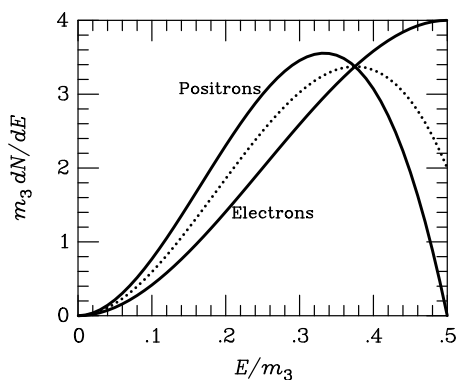


FIG. 3. Positron and electron spectrum for  $\nu_3 \rightarrow \nu_1 e^+ e^-$  according to Eq. (3) for a Dirac neutrino with  $m_3 \gg m_e$ . The dotted line is the average between the two spectra which pertains to both  $e^+$  and  $e^-$  when  $\nu_3$  is a Majorana particle.

For a parent neutrino mass  $m_3 \gg m_e$  these spectra are shown in Fig. 3. For  $\bar{\nu}_3$  the role of electrons and positrons is interchanged. For a Majorana parent the electron and positron spectra are the same. Each is the average of the Dirac spectra of Eq. (3)—see the dotted line in Fig. 3.

### III. BREMSSTRAHLUNG

#### A. Matrix Element

For a Dirac neutrino the amplitude for  $\nu_3 \rightarrow \nu_1 e^+ e^- \gamma$  is given by the Feynman graph of Fig. 1(a) with a photon attached to either the electron or positron line. We calculate the squared matrix element, summed over all final-state spin and polarization states. However, because relativistic Dirac neutrinos are produced primarily with negative helicities we do not average over the initial-state helicities—a helicity-averaged rate would not pertain to a realistic source. We find

$$\begin{aligned} \sum_{\substack{\text{final-state spins} \\ \text{polarizations}}} |\mathcal{M}|^2 &= \left( \frac{e G_F}{\sqrt{2}} \right)^2 |U_{e1} U_{e3}|^2 \\ &\times \frac{8}{C_{\gamma-}^2} \left( C_{\gamma-} C_{3+} C_{1\gamma} - C_{1-} C_{3+} m_e^2 - C_{3+} C_{1\gamma} m_e^2 \right) \\ &+ \frac{8}{C_{\gamma+}^2} \left( C_{1-} C_{\gamma+} C_{3\gamma} - C_{1-} C_{3+} m_e^2 - C_{1-} C_{3\gamma} m_e^2 \right) \\ &+ \frac{8}{C_{\gamma-} C_{\gamma+}} \left( 2C_{-+} C_{1-} C_{3+} + C_{-+} C_{1-} C_{3\gamma} \right. \\ &\quad \left. + C_{-+} C_{3+} C_{1\gamma} - C_{3-} C_{1-} C_{\gamma+} + C_{1-} C_{\gamma-} C_{3+} \right. \\ &\quad \left. + C_{1-} C_{3+} C_{\gamma+} - C_{\gamma-} C_{3+} C_{1+} \right), \end{aligned} \quad (4)$$

where  $C_{1+} \equiv P'_1 P'_+$  and so forth with  $P'_{1,+,-,\gamma} = P_{1,+,-,\gamma}$  the four momenta of  $\nu_1$ ,  $e^+$ ,  $e^-$ , and  $\gamma$ , respectively. Only for the parent neutrino we have  $P'_3 = P_3 - m_3 S_3$  with  $S_3$  its spin four vector; we have not summed over its helicities. In the  $\nu_3$  rest frame  $P'_3 = m_3(1, -\mathbf{s}_3)$  with  $\mathbf{s}_3$  a unit vector in the spin direction of  $\nu_3$ .

If the initial state is a Dirac antineutrino we find the same squared matrix element with the role of  $e^+$  and  $e^-$  interchanged. Moreover, we then have  $P'_3 = P_3 + m_3 S_3$ , leading to  $P'_3 = m_3(1, +\mathbf{s}_3)$  in the  $\bar{\nu}_3$  rest frame. A simple CP transformation reveals that the photon angular distribution relative to the spin-polarization vector is opposite compared to that of a neutrino. Put another way, neutrinos and antineutrinos with the same momentum but opposite helicities will produce identical angular photon distributions relative to the momentum direction.

For Majorana neutrinos the squared matrix element is the sum of Eq. (4) with the same expression under the exchange of  $e^+$  with  $e^-$ . In this case the photon angular distribution in the parent rest frame is isotropic, independently of its helicity state. For Majorana neutrinos, then, one may average over the initial-state neutrino helicities (one may use  $P'_3 = P_3$ ) without loss of generality.

#### B. Photon Spectrum

In order to calculate the photon spectrum we need to integrate over the four-body final-state phase space, leaving only the  $d\omega$  integration undone, where  $\omega$  is the photon energy. The shape of the photon spectrum, integrated over all emission angles, is the same for Dirac neutrinos or antineutrinos as well as for Majorana neutrinos, independently of their polarization state. We have performed the phase-space integration numerically by a Monte Carlo technique with the parametrization outlined in Appendix A.

To derive a useful representation of the resulting spectrum we borrow from a standard result for the classical spectrum of an inner bremsstrahlung process [15]

$$\frac{d\Gamma}{d\omega} = \frac{\Gamma_{\text{bare}}}{\omega} \frac{\alpha}{\pi} \left[ \frac{1}{v} \ln \left( \frac{1+v}{1-v} \right) - 2 \right], \quad (5)$$

where  $\omega$  is the photon energy,  $\Gamma_{\text{bare}}$  the rate for the bare process,  $\alpha \approx 1/137$  the fine-structure constant, and  $v$  the speed of the produced charged lepton. This calculation applies to a process like beta decay where the recoiling nucleus does not contribute to the bremsstrahlung rate. In our case we have two charged leptons so that we expect twice this rate, for the moment ignoring interference effects. Of course, the  $1/\omega$  divergence represents the well-known infra-red bremsstrahlung behavior.

Motivated by this classical result we represent the photon spectrum by

$$\frac{d\Gamma}{d\omega} = \frac{\Gamma_{\text{bare}}}{\omega} \frac{2\alpha}{\pi} A g(x), \quad (6)$$

where  $g(x)$  is a dimensionless function which depends on the parent neutrino mass  $m_3$ . The dimensionless coefficient  $A$  is factored out such that  $g(0) = 1$ , i.e.  $g(x)$  describes the spectral shape, not its absolute amplitude. The factor  $\Gamma_{\text{bare}}$  includes a global factor of 2 for Majorana neutrinos as discussed in section II. The dimensionless photon energy  $x \equiv \omega/\omega_{\text{max}}$  is in the range  $0 \leq x \leq 1$ , where

$$\omega_{\text{max}} = \frac{m_3}{2} \left[ 1 - \left( \frac{2m_e}{m_3} \right)^2 \right] \quad (7)$$

is the end point of the photon spectrum.

In the upper panel of Fig. 4 we show  $g(x)$  for several values of  $m_3$ . For all cases  $g(x)$  decreases monotonically from 1 at  $x = 0$  to 0 at  $x = 1$ . This behavior suggests a power-law representation

$$g(x) = (1-x)^{p(x)}, \quad (8)$$

where the power-law index  $p(x)$  is itself a slowly varying function of  $x$ . We show it in the lower panel of Fig. 4 for several values of  $m_3$ . In a practical application it would probably be enough to use a constant, typical value for  $p$ . For reference we show in the upper panel as a dotted

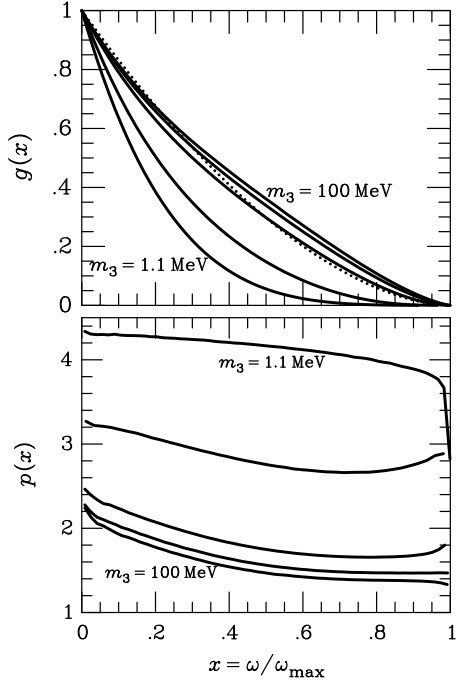


FIG. 4. *Upper Panel:* Numerical results for the dimensionless bremsstrahlung photon spectrum  $g(x)$  as defined in Eq. (6) for parent neutrino masses  $m_3 = 1.1, 2, 10, 30$ , and  $100$  MeV (bottom to top). The dotted line is a power law of the form Eq. (8) with  $p = 1.75$ . *Lower Panel:* Power-law index  $p(x)$  as defined in Eq. (8) for the same parent masses (top to bottom).

line  $g(x)$  for a fixed value  $p = 1.75$  which would appear to produce a reasonably good approximation if  $m_3$  is taken to be around  $10$  MeV.

The dimensionless coefficient  $A$  measures the zero-point intercept of the spectrum. Numerical values for several parent masses are given in Table I.

It is a useful check of our calculation to compare these numerical values with the classical result Eq. (5) which should be exact in the limit of soft photons. However, it does not include the interference between the radiation emitted by both final-state charged leptons. What we list in Table I as the classical prediction, then, is the incoherent sum of the expected radiation power from the final-state electron and positron where we have integrated over the velocity distribution of these particles as

TABLE I. Values for the coefficient  $A$  as defined in Eq. (6).

$m_3$ [MeV]	$A$ (quantum)	$A$ (classical)
100.0	7.99	7.55
30.0	5.58	5.16
10.0	3.44	3.06
2.0	0.76	0.54
1.1	0.068	0.036

given by the bare process in Eq. (3). This classical result is always smaller, indicating that the interference effect is constructive on average. In any case, for high parent masses the importance of interference disappears as one would have expected because then the bremsstrahlung photons are primarily emitted co-linear with the charged leptons so that the overlap of the two “bremsstrahlung cones” becomes small. The most important conclusion is that we do not seem to have lost factors of  $2, \pi$ , and so forth in the course of our calculation.

### C. Angular Distribution

The photon angular distribution is isotropic for Majorana neutrinos while it is nontrivial in the Dirac case. A possible angular distribution can arise only from the terms  $C_{3\gamma} = (P_3 - m_3 S_3)P_\gamma$  in the squared matrix element Eq. (4). Because it is linear in  $C_{3\gamma}$  it is clear that after all unobserved phase-space degrees of freedom have been integrated out we are left with a term which is independent of the angle  $\theta$  between the photon momentum and the spin-direction, and one that is proportional to  $\cos \theta$ . (The signs are chosen such that  $\cos \theta = +1$  corresponds to the direction along the parent spin.) Thus for a fixed photon energy  $\omega$  the most general normalized angular distribution is of the form

$$\frac{dN_\gamma}{d\cos \theta} = \frac{1 + a \cos \theta}{2} \quad (9)$$

where  $-1 \leq a \leq +1$ . Again, because  $\theta$  is measured relative to the spin direction, we have  $a \rightarrow -a$  for antineutrinos. For Majorana neutrinos we have  $a = 0$  for all  $\omega$  as mentioned above.

In Fig. 5 we show  $a$  as a function of the dimensionless photon energy  $x = \omega/\omega_{\max}$  for several choices of parent neutrino mass. Contrary to what one might have expected the angular distribution depends very sensitively on the photon energy. Soft photons are emitted nearly isotropically, with a slight bias in the spin direction. The

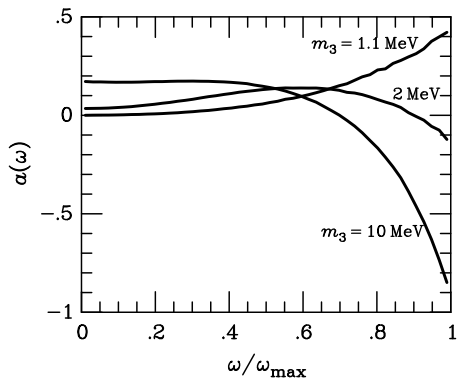


FIG. 5. Photon angular-distribution parameter  $a(x)$  as defined in Eq. (9) for several choices of parent neutrino mass.

highest-energy photons are emitted dominantly against the spin direction if  $m_3 \gg m_e$ . In the limit  $m_3 \rightarrow \infty$  it is easy to show analytically that  $a = -1$  for  $x = 1$ . (The reverse for antineutrinos.)

#### IV. DISCUSSION AND SUMMARY

We have calculated the rate, photon spectrum, and photon angular distribution of the inner bremsstrahlung process  $\nu_\tau \rightarrow \nu_e e^+ e^- \gamma$  which could have produced a  $\gamma$  ray burst from SN 1987A, contrary to several observations. Therefore, one can derive limits on the relevant neutrino mixing angle even though the most relevant data, the 1991 COMPTEL observations of SN 1987A [12], have not yet been used in this regard.

After assuming a certain magnitude and spectrum of the primary  $\nu_\tau$  and  $\bar{\nu}_\tau$  flux, a prediction of the bremsstrahlung photon flux and spectrum depends on the photon energy distribution as well as their angular distribution relative to the neutrino momentum.

The simplest case is that of Majorana neutrinos where the angular distribution in the neutrino rest frame is isotropic, independently of the parent polarization. The rough estimate of the bremsstrahlung rate that had been used in previous papers is  $d\Gamma/d\omega = (\alpha/\pi) \Gamma_{\text{bare}}/\omega$  with photon energies  $\omega$  up to half the parent neutrino mass. It was overlooked that for Majorana neutrinos  $\Gamma_{\text{bare}}$  is twice that of Dirac neutrinos. We have a further factor 2 because bremsstrahlung arises from two final-state charged leptons. Finally, one gains the factor 4 which is given in Table I. For example, taking  $m_{\nu_\tau} = 10$  MeV one gains overall more than a factor of 10. However, the spectrum decreases somewhat faster with  $\omega$  than had been assumed.

Therefore, the previous limits on the mixing angle will improve accordingly. They would improve much further by applying our results to the COMPTEL data which encompass a much larger viewing period than the previously used SMM and PVO data. It would be an important future project to analyse the COMPTEL data with regard to the  $\nu_\tau \rightarrow \nu_e e^+ e^- \gamma$  decay!

Dirac neutrinos exhibit a nontrivial photon angular distribution if they are polarized. Because the  $\nu_\tau$ 's and  $\bar{\nu}_\tau$ 's emitted from a SN have opposite polarizations, the anisotropy of the photon distribution does not cancel between them. On the other hand, for a mass in the 10 MeV range and typical energies of around 30 MeV they are not particularly relativistic so that their degree of polarization is incomplete. For smaller masses the degree of polarization is stronger, but the deviation from isotropy is less pronounced. A detailed treatment of the Dirac case is probably too complicated to be worth conducting in view of the many uncertainties with regard to the overall neutrino flux and spectrum.

We do not believe that interpreting, for example, the COMPTEL data requires an implementation of our

bremsstrahlung results in every detail. (One would need numerical results on a finely spaced grid of parameters.) Rather, we think that our results should be used as a basis for an approximate treatment where the magnitude of the possible errors is understood and controlled.

Independently from the SN application, the bremsstrahlung process features differences between Dirac and Majorana neutrinos which are interesting in their own right.

#### ACKNOWLEDGMENTS

This work is based on a thesis submitted by H.S. to the Ludwig-Maximilians-Universität, München, in partial fulfillment of the requirements for a *Diplom* degree (Master of Science). Partial support by the Deutsche Forschungsgemeinschaft under grant No. SFB 375 is acknowledged.

#### APPENDIX A: PHASE-SPACE INTEGRATION

We give some details about the integration of the four-particle phase space in the  $\nu_3 \rightarrow \nu_1 e^+ e^- \gamma$  process. Following Ref. [16] a four-body phase-space integral can be transformed according to

$$\begin{aligned} & \int \prod_{i=1}^4 \frac{d^3 \mathbf{p}_i}{2E_i} \delta^4 \left( P_{\text{ini}} - \sum_{i=1}^4 P_i \right) \\ &= \frac{\pi}{256} \int \frac{\sqrt{\lambda(s, s_a, s_b)}}{s} \frac{\sqrt{\lambda(s_a, m_1^2, m_2^2)}}{s_a} \\ & \quad \times \frac{\sqrt{\lambda(s_b, m_3^2, m_4^2)}}{s_b} ds_a ds_b d\cos\theta d\Omega_a d\Omega_b, \end{aligned} \quad (\text{A1})$$

with the four momenta  $P_i = (E_i, \mathbf{p}_i)$ ,  $i = 1, \dots, 4$ , and the masses  $m_i^2 = P_i^2$ . Further, we use

$$\lambda(a, b, c) = a^2 + b^2 + c^2 - 2ab - 2ac - 2bc. \quad (\text{A2})$$

The four particles have been grouped into two subsystems with  $s_a = (P_1 + P_2)^2$  and  $s_b = (P_3 + P_4)^2$  while  $s^2 = (P_1 + P_2 + P_3 + P_4)^2 = m_{\text{ini}}^2$ . The angles  $\Omega_{a,b}$  are within the CM frames of the two subsystems while  $\theta$  is the angle with which the two subsystems move in opposite directions relative to some chosen direction in the overall CM frame, i.e. in the rest frame of the decaying particle, for example relative to its spin. The limits of integration are

$$\begin{aligned} (m_1 + m_2)^2 &\leq s_a \leq (\sqrt{s} - m_3 - m_4)^2, \\ (m_3 + m_4)^2 &\leq s_b \leq (\sqrt{s} - \sqrt{s_1})^2. \end{aligned} \quad (\text{A3})$$

Finally we need to express the original four momenta  $P_i$  in terms of the new integration variables. Assuming that the two subsystems move in opposite directions along the  $z$ -axis we find in the CM frame

$$P_1 = \begin{pmatrix} \gamma_a^0 E_1^R + \gamma_a p_a^R \cos \theta_a \\ p_a^R \sin \theta_a \cos \phi_a \\ p_a^R \sin \theta_a \sin \phi_a \\ \gamma_a^0 p_a^R \cos \theta_a + \gamma_a E_1^R \end{pmatrix} \quad (\text{A4})$$

and

$$P_2 = \begin{pmatrix} \gamma_a^0 E_2^R - \gamma_a p_a^R \cos \theta_a \\ -p_a^R \sin \theta_a \cos \phi_a \\ -p_a^R \sin \theta_a \sin \phi_a \\ -\gamma_a^0 p_a^R \cos \theta_a + \gamma_a E_2^R \end{pmatrix} \quad (\text{A5})$$

with

$$\begin{aligned} E_1^R &= \frac{s_a + m_1^2 - m_2^2}{2\sqrt{s_a}}, \\ E_2^R &= \frac{s_a + m_2^2 - m_1^2}{2\sqrt{s_a}}, \\ p_a^R &= \frac{1}{2} \sqrt{\frac{\lambda(s_a, m_1^2, m_2^2)}{s_a}}. \end{aligned} \quad (\text{A6})$$

The boost-factors are

$$\begin{aligned} \gamma_a^0 &= \frac{s + s_a - s_b}{2\sqrt{ss_a}}, \\ \gamma_a &= \frac{\sqrt{\lambda(s, s_a, s_b)}}{2\sqrt{ss_a}}. \end{aligned} \quad (\text{A7})$$

For the other subsystem we have

$$P_3 = \begin{pmatrix} \gamma_b^0 E_3^R - \gamma_b p_b^R \cos \theta_b \\ p_b^R \sin \theta_b \cos \phi_b \\ p_b^R \sin \theta_b \sin \phi_b \\ \gamma_b^0 p_b^R \cos \theta_b - \gamma_b E_3^R \end{pmatrix} \quad (\text{A8})$$

and

$$P_4 = \begin{pmatrix} \gamma_b^0 E_4^R + \gamma_b p_b^R \cos \theta_b \\ -p_b^R \sin \theta_b \cos \phi_b \\ -p_b^R \sin \theta_b \sin \phi_b \\ -\gamma_b^0 p_b^R \cos \theta_b - \gamma_b E_4^R \end{pmatrix}. \quad (\text{A9})$$

The energies and boost factors are the same as before with the substitutions  $a \leftrightarrow b$ ,  $1 \rightarrow 3$  and  $2 \rightarrow 4$ .

---

- [4] N. de Leener-Rosier et al., Phys. Lett. B **177**, 228 (1986).
- [5] D.A. Bryman et al., Phys. Rev. Lett. **50**, 1546 (1983).
- [6] C. Hagner et al., Phys. Rev. D **52**, 1343 (1995).
- [7] D. Toussaint and F. Wilczek, Nature **289**, 777 (1981).
- [8] A. Dar, J. Goodman and S. Nussinov, Phys. Rev. Lett. **58**, 2146 (1987).
- [9] R.N. Mohapatra, S. Nussinov and X. Zhang, Phys. Rev. D **49**, 3434 (1994).
- [10] G. Raffelt, *Stars as Laboratories for Fundamental Physics*, (Chicago University Press, Chicago, 1996).
- [11] A. Dar and S. Dado, Phys. Rev. Lett. **59**, 2368 (1987).
- [12] L. Oberauer et al., Astropart. Phys. **1**, 377 (1993).
- [13] A.H. Jaffe and M.S. Turner, Phys. Rev. D **55**, 7951 (1997).
- [14] R.S. Miller, *A Search for Radiative Neutrino Decay and Its Potential Contribution to the Cosmic Diffuse Gamma-Ray Flux* (Ph.D. Thesis, Univ. New Hampshire, Dec. 1995). R.S. Miller, J.M. Ryan and R.C. Svoboda, Astron. Astrophys. Suppl. Ser. **120**, 635 (1996).
- [15] R.E. Shrock, Phys. Rev. D **24**, 1275 (1981).
- [16] L.F. Li and F. Wilczek, Phys. Rev. D **25**, 143 (1982).
- [17] J.D. Jackson, *Classical Electrodynamics*, 2nd ed. (John Wiley, New York, 1975).
- [18] T. Bardin and T. Riemann, Nucl. Phys. B **462**, 3 (1996).

---

- [1] E.W. Kolb and M.S. Turner, *The Early Universe* (Addison-Wesley, Reading, Mass., 1990).
- [2] D. Buskulic et al. (ALEPH Collaboration), Phys. Lett. B **349**, 585 (1995). R. Barate et al. (ALEPH Collaboration), Report CERN-PPE-97-138 (Oct. 1997), submitted to Z. Phys. C.
- [3] J. Bardeen, J. Bond and G. Efstathiou, Astrophys. J. **321**, 28 (1987). J.R. Bond and G. Efstathiou, Phys. Lett. B **265**, 245 (1991). S. Dodelson, G. Gyuk and M.S. Turner, Phys. Rev. Lett. **72**, 3754 (1994). M. White, G. Gelmini and J. Silk, Phys. Rev. D **51**, 2669 (1995). S. Dodelson, E.I. Gates and M.S. Turner, Science **274**, 69 (1996).